Macromolecular Chemistry and Physics
www.mcp-journal.de

Phase Diagram of Tapered Copolymers Based on Isoprene and Styrene

Eftyxis Galanos, Christian Wahlen, Hans-Juergen Butt, Holger Frey, and George Floudas**

Although several phase diagrams of block copolymers prepared by sequential monomer addition are known today, the phase diagrams of the corresponding tapered copolymers have not been reported in detail and this despite the industrial importance of the latter. A phase diagram based on a series of tapered diblock copolymers is reported, generated by the *sec*-butyllithium initiated statistical anionic copolymerization of styrene and isoprene in cyclohexane. This affords copolymers with polyisoprene volume fractions, *f*, in the range of $0.43 < f < 0.82$ and total molar mass in the range of 46–160 kg mol^{-1}. The phase diagram consists of lamellae, hexagonally packed cylinders, weakly ordered hexagonally packed cylinders (CYL), and perforated (PL) as well as irregular bicontinuous morphologies. The phase state in the tapered copolymers bears some similarities and several distinct differences in comparison to the respective copolymers prepared by conventional sequential monomer addition. It is shown that the weakly ordered CYL/PL morphologies comprise a large part of the phase diagram that is significantly extended in comparison to diblock copolymers prepared sequentially. On the other hand, the composition range for the bicontinuous morphologies is similar in the two systems ($0.64 < f_{PI} < 0.68$).

1. Introduction

Thermoplastic elastomers are melt-processable elastic materials.[1] They are based on anchoring a rubbery center block between two glassy end blocks. Well-known examples are triblock copolymers of poly(styrene-*b*-isoprene-*b*-styrene) (SIS) and poly(styrene-*b*-butadiene-*b*-styrene) (SBS) (respective trade names Dexco and Kraton).[2,3] Industrial processing of such copolymers, by, e.g., high-speed melt extrusion, requires an accessible disordered phase, where the melt viscosity is low. This requirement suggests lowering of the order-to-disorder transition temperature, T_{ODT}, while maintaining an ordered state at ambient temperature that provides the desired mechanical properties. Given that one block is the glassy polystyrene, this practically suggests that T_{ODT} should be in the range: $T_g^{PS} < T_{ODT} < T_{decomposition}$. The disordering temperature in block copolymers is controlled—to a large extent—by the product χN, where χ is the interaction parameter, N is the total degree of polymerization, and the volume fraction, f. For a given copolymer, reducing T_{ODT} requires lowering N.[4,5] However, by lowering N, chains become unentangled and as a consequence the respective materials exhibit poor mechanical properties.

A more efficient way of reducing the T_{ODT} while maintaining an entangled state, is by decreasing the effective interaction parameter, e.g., by controlling the interfacial mixing of the two polymers. Indeed, block copolymers with a controlled tapering across the interface can provide access to higher molar mass diblock copolymers that reside in the weak-segregation limit.[6–10] Recent efforts in this direction that rely on online-monitoring of copolymer formation by in situ NMR or NIR techniques gave access to tapered block copolymers by copolymerizing mixtures of styrene and isoprene in cyclohexane.[11–14] The highly disparate reactivity rations of I and S in this solvent ($r_I = 12.8$ and $r_S = 0.05$)[13,14] lead to well-defined tapered diblock copolymers. In a second step, repeated

E. Galanos
Department of Physics
University of Ioannina
P.O. Box 1186, Ioannina 451 10, Greece

C. Wahlen, H. Frey
Department of Chemistry
Johannes Gutenberg Universität Mainz
55099 Mainz, Germany
E-mail: hfrey@uni-mainz.de

H.-J. Butt, G. Floudas
Max Planck Institute for Polymer Research
55128 Mainz, Germany

G. Floudas
Department of Physics
University of Ioannina
P.O. Box 1186, Ioannina 451 10, Greece
E-mail: gfloudas@uoi.gr

G. Floudas
University Research Center of Ioannina (URCI) – Institute of Materials Science and Computing
Ioannina 45110, Greece

The ORCID identification number(s) for the author(s) of this article can be found under https://doi.org/10.1002/macp.202200033

© 2022 The Authors. Macromolecular Chemistry and Physics published by Wiley-VCH GmbH. This is an open access article under the terms of the Creative Commons Attribution-NonCommercial-NoDerivs License, which permits use and distribution in any medium, provided the original work is properly cited, the use is non-commercial and no modifications or adaptations are made.

DOI: 10.1002/macp.202200033

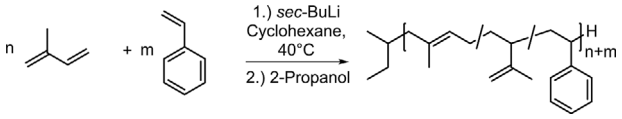

Scheme 1. Synthetic strategy used for the tapered P(I-co-S) copolymers.

addition of monomers was employed in preparing nearly symmetric tapered multiblock copolymers with a molar mass of up to 400 kg mol^{-1} and the expected lamellar morphology.[11] Results by X-ray scattering and transmission electron microscopy indicated weakly ordered lamellae at ambient temperature. The domain spacing, d, was found to scale as $d \approx N^{0.62}$, suggesting stretching of chains and non-ideal configurations. Temperature-dependent small-angle X-ray scattering (SAXS) revealed that the tapered multiblock copolymers undergo a fluctuation-induced first-order transition at the respective T_{ODT}.[11] In addition, the copolymers were shown to combine nanophase separation with excellent mechanical properties (toughness and strain at break exceeding 900%). Another study[15] explored ways of enhancing the poor tensile properties of tapered *diblock* copolymers, namely by blending them with tapered *multiblock* copolymers. The results demonstrated strongly enhanced elastic response and toughness by blending a small amount of tapered multiblock copolymer with the tapered diblock copolymer while retaining an ordered morphology.[15]

Despite several recent studies on tapered P(I-*co*-S) copolymers, the effective phase diagram has not been explored in detail. Herein we employ 20 tapered P(I-*co*-S) diblock copolymers with polyisoprene volume fractions in the range $0.43 < f < 0.82$ and total molar mass from 46 to 160 kg mol^{-1} and investigate the morphology by SAXS and the viscoelastic behavior by rheology. We found that the weakly ordered hexagonally packed cylinder and perforated morphologies comprise a larger part of the phase diagram in the case of the tapered copolymers.

2. Experimental Section

2.1. Synthesis

For the synthesis of the tapered copolymers of isoprene and styrene, the procedure described in refs. [11,13] and shown in **Scheme 1** was followed. **Table 1** contains the theoretical values for the molar fraction of isoprene for each copolymer ($x_{isoprene}^{th}$), as well as the molar fraction as determined by ^{1}H NMR spectra (**Figure 1**).[14] The determined molar fractions fit very well to the theoretical values. The tapered structure was simulated (**Figure 2**) based on the reactivity ratios given in the publication of Quinebéche et al. ($r_{isoprene} = 0.05$, $r_{styrene} = 12.8$, determined at 40 °C).[14] The volume fraction at the inflection point of the gradient structure was determined form the molar fractions of NMR spectroscopy and used subsequently in the phase diagram. Therefore, a transformation of the molar composition profile to the volume composition profile was performed, like reported in previous work.[16] The molecular weights, determined by SEC (shown in Table 1), are overestimated, caused by the PS calibration. It is known from the previous works, that the PS standard typically overestimates the molecular weights of P(I-co-S) copolymers.[11–13] In addition, errors caused by dosing, due to the low amounts of initiator, and irreversible termination of

Table 1. Characterization data of synthesized tapered copolymers of isoprene and styrene with varying monomer ratio and molecular weight.

Sample	M_n^{th} [kg mol^{-1}]	$M_n^{a)}$ [kg mol^{-1}]	$Đ^{a)}$	$x_{isoprene}^{th}$	$f_{PI,infl.}^{th}$	$x_{isoprene}^{b)}$	$f_{PI,infl.}^{b)}$
SI-51-67	40	50.9	1.13	0.63	0.67	0.62	0.67
SI-46-68	40	46.3	1.10	0.65	0.69	0.64	0.68
SI-53-71	40	52.7	1.09	0.67	0.71	0.67	0.71
SI-46-72	40	46.1	1.16	0.69	0.73	0.68	0.72
SI-59-71	40	58.8	1.17	0.68	0.72	0.67	0.71
SI-73-71	60	72.9	1.09	0.68	0.72	0.67	0.71
SI-57-67	60	57	1.16	0.67	0.71	0.62	0.67
SI-55-66	60	55.2	1.13	0.69	0.73	0.61	0.66
SI-112-67	80	111.6	1.08	0.64	0.68	0.63	0.67
SI-97-69	80	96.8	1.06	0.66	0.7	0.65	0.69
SI-101-71	80	101.4	1.06	0.68	0.72	0.67	0.71
SI-118-73	80	118.4	1.08	0.7	0.74	0.69	0.73
SI-140-75	120	139.9	1.07	0.72	0.76	0.71	0.75
SI-160-73	120	159.7	1.08	0.7	0.74	0.69	0.73
SI-155-71	120	154.7	1.09	0.68	0.72	0.67	0.71
SI-130-82	120	130.3	1.07	0.8	0.83	0.79	0.82
SI-137-80	120	137.1	1.08	0.78	0.81	0.77	0.8
SI-134-78	120	134.3	1.10	0.76	0.79	0.75	0.78
SI-128-76	120	127.5	1.07	0.74	0.77	0.72	0.76
SI-253-43	240	252.9	1.08	0.4	0.43	0.4	0.43

[a)] Determined by SEC measurements in THF at 25 °C with PS standard; [b)] Determined by ^{1}H NMR spectra (400 MHz, C_6D_{12}). $x_{isoprene}$: molar fraction of isoprene, $f_{PI,infl.}$: volume fraction of polyisoprene phase at the inflection point.

© 2022 The Authors. Macromolecular Chemistry and Physics published by Wiley-VCH GmbH

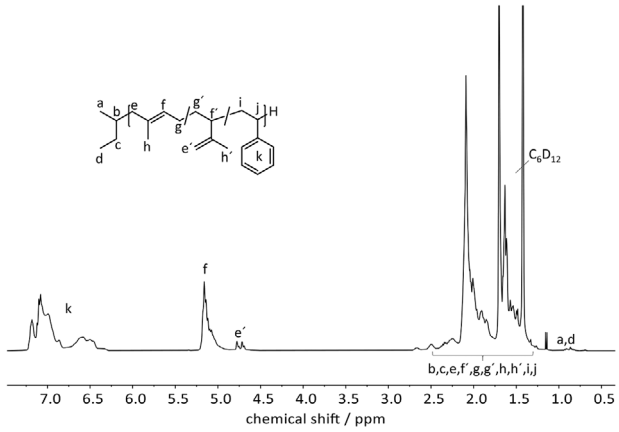

Figure 1. ^{1}H NMR spectrum (400 MHz, C_6D_{12}) of a tapered isoprene/styrene copolymer (SI-46-72).

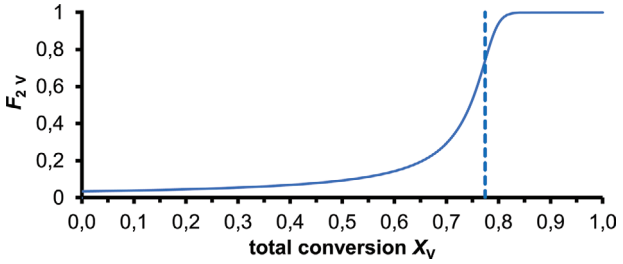

Figure 2. Simulation of the tapered structure of an isoprene/styrene copolymer (SI-128-76), showing the instantaneous styrene volume incorporation (F_{2v}) in dependence of the polymer volume fraction (Xv), as reported in previous work.[16] The dashed line indicates the inflection point of the gradient ($f_{PI,infl.}$).

the initiator (which is rather unlikely) have to be considered. For example, the lower molecular weights of the samples SI-55-66 and SI-57-67 are caused by dosing errors.

2.2. Determination of $x_{isoprene}$

The molar fraction of isoprene in the P(I-co-S) copolymers was calculated from the integrals (I) of the proton signals é, f and k of the ^{1}H NMR spectrum (Figure 1) as follows:

$$x_{\text{isoprene}} = \frac{I(f) + \frac{I(e')}{2}}{I(k) + I(f) + \frac{I(e')}{2}} \quad (1)$$

2.3. Small-Angle X-Ray Scattering

Small-angle (SAXS) measurements were made using CuKα radiation (RigakuMicroMax 007 x-ray generator, Osmic Confocal Max-Flux curved multilayer optics). 2D diffraction patterns were recorded on an Mar345 image plate detector at a sample-detector distance of 2076 mm. Intensity distributions as a function of the modulus of the total scattering vector, $q = (4\pi/\lambda)\sin(2\theta/2)$, where 2θ is the scattering angle, were obtained by radial averaging of the 2D datasets. Samples in the form of thick films (≈1 mm) were prepared by slow solvent casting. Temperature-dependent measurements of 1 h long were made by heating the films from 293 to 453 K in 10 K steps followed by 1 h equilibration at each temperature and subsequent cooling aiming at obtaining the structure factor and further identifying the corresponding order-to-disorder transition temperatures.

2.4. Rheology

A TA Instruments, AR-G2, with a magnetic bearing that allows for nanotorque control was used for recording the viscoelastic properties of the tapered (and sequential) copolymers. Measurements were made with the environmental test chamber (ETC) as a function of temperature and frequency. Samples were prepared on the lower rheometer plate (8 and 25 mm). Then the upper plate was brought into contact, and the gap thickness was adjusted. The linear and nonlinear viscoelastic regimes were identified by recording the complex shear modulus $|G^*|$ at $\omega = 10$ rad s^{-1} as a function of shear rate. The strain amplitude was typically below 1% to avoid non-linearities. Subsequent experiments involved (i) isochronal temperature ramps with $\omega = 1$ rad s^{-1} at a rate of 1 K min^{-1} between 343 and 523 K and (ii) isothermal frequency scans within the range $3 \times 10^{-2} < \omega < 10^2$ rad s^{-1} at several temperatures, and (iii) isochronal and isothermal time scans (ordering kinetics) at carefully selected temperatures by following the evolution of the storage and loss moduli ($\omega = 0.5$ rad s^{-1}). The latter experiment was followed by slow isochronal heating (rate 0.2 K min^{-1}) in order to locate the apparent disordering temperature.

3. Results and Discussion

3.1. Small-Angle X-Ray Scattering

The phase state of the different copolymers was determined via SAXS experiments. Typically, samples were heated from ambient temperature to 453 K, and SAXS curves were recorded at intermediate temperatures. The SAXS results are summarized in **Table 2**.

Some representative SAXS curves are depicted in **Figure 3**; additional SAXS data are presented in Figures S1–S7 (Supporting Information). We start with a nearly symmetric tapered diblock copolymer SI-253-43 with $f_{PI} = 0.43$ investigated earlier by us.[11] Bragg reflections at q ratios of 1:2:3:5 reveal a lamellar (LAM) morphology with a periodicity of 74 nm (at 303 K) as $d_0 = 2\pi/q^*$, where q^* is the modulus of the scattering vector corresponding to the first Bragg reflection. The SAXS results for the symmetric copolymers are in agreement with TEM results (Figure S8, Supporting Information).[12,15] For SI-118-73 ($f_{PI} = 0.73$) at 453 K, reflections have relative q values of $1:3^{1/2}:4^{1/2}:7^{1/2}:9^{1/2}$ revealing an ordered hexagonally packed cylindrical structure (HPC) with periodicity of 43 nm and inter-cylinder distance of 49.7 nm ($d = d_0(4/3)^{1/2}$). For SI-97-69 ($f_{PI} = 0.69$) at 453 K reflections with relative q values of $1:3^{1/2}:7^{1/2}:9^{1/2}$ are still present, but with lower intensity relative to the primary reflection suggesting weakly ordered hexagonally packed cylindrical or a perforated morphology (CYL/PL) with periodicity of 38.1 nm. For SI-46-68 ($f_{PI} = 0.68$) at 423 K, reflections appear at a q ratio of $3^{1/2}:4^{1/2}$ suggestive of a bicontinuous morphology without long-range order (it resembles to the double gyroid morphology with the Ia$\bar{3}$d

© 2022 The Authors. Macromolecular Chemistry and Physics published by Wiley-VCH GmbH

Table 2. Phase state of the tapered diblock copolymers based on SAXS.

Sample code	$f_{PI,\ infl}$	Phase state
SI-51-67	0.67	LAM up to 413; BIC up to 453 K
SI-46-68	0.68	BIC up to 433 K; $T_{ODT} = 453 \pm 5$ K
SI-53-71	0.71	HPC up to 453 K; $T_{ODT} = 455 \pm 2$ K
SI-46-72	0.72	HPC up to 453 K; $T_{ODT} = 453 \pm 5$ K
SI-59-71	0.71	HPC up to 453 K
SI-73-71	0.71	HPC up to 453 K; T_{ODT} not accessible (n.a.)
SI-57-67	0.67	LAM up to 363 K; T_{ODT} n.a.
SI-55-66	0.66	LAM up to 363 K; T_{ODT} n.a.
SI-112-67	0.67	CYL/PL up to 453 K; T_{ODT} n.a.
SI-97-69	0.69	CYL/PL up to 453 K; T_{ODT} n.a.
SI-101-71	0.71	HPC up to 453 K; T_{ODT} n.a.
SI-118-73	0.73	HPC up to 453 K; T_{ODT} n.a.
SI-140-75	0.75	HPC up to 453 K; T_{ODT} n.a.
SI-160-73	0.73	HPC up to 453 K; T_{ODT} n.a.
SI-155-71	0.71	CYL/PL up to 453 K; T_{ODT} n.a.
SI-130-82	0.82	HPC up to 453 K; T_{ODT} n.a.
SI-137-80	0.80	HPC up to 453 K; T_{ODT} n.a.
SI-134-78	0.78	HPC up to 453 K; T_{ODT} n.a.
SI-128-76	0.76	HPC up to 453 K; T_{ODT} n.a.
SI-253-43	0.43	LAM

LAM: lamellar; HPC: hexagonally packed cylinders; CYL: weakly ordered hexagonally packed cylinders; PL: perforated; BIC: irregular bicontinuous morphology, n.a. for not accessible.

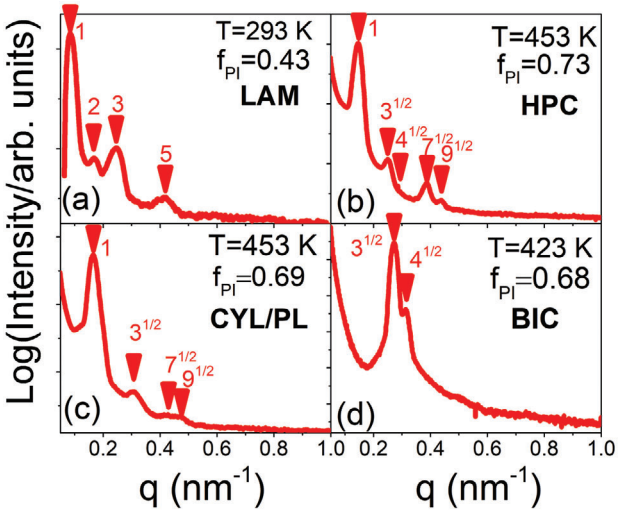

Figure 3. Representative SAXS patterns of the P(I-*co*-S) copolymers. The arrows give positions of Bragg peaks corresponding to a) lamellar (LAM) in SI-253-43, b) ordered hexagonally packed cylindrical structure (HPC) in SI-118-73, c) a weakly ordered hexagonally packed cylindrical or perforated morphology (CYL/PL) in SI-97-69, and d) a bicontinuous (BIC/G) morphology without long-range order in SI-46-68.

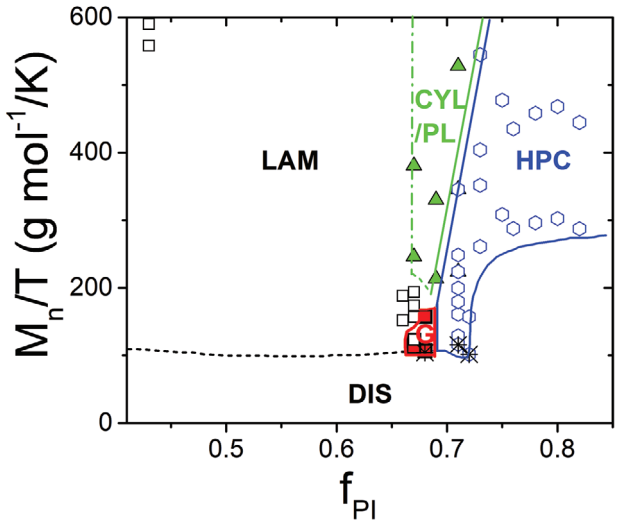

Figure 4. Phase diagram for tapered P(I-*co*-S) copolymers based on SAXS, showing the presence of lamellae (LAM) (black squares), hexagonally packed cylinders (HPC) (blue hexagons), weakly ordered cylinders (CYL) and perforated layers (PL) (green triangles) and bicontinuous (BIC/G) (red squares) morphologies. The order-to-disorder transition temperatures (*) are also shown. Lines give the boundaries between the different morphologies as guide to the eye.

space group symmetry). It should be mentioned that the double gyroid morphology was reported earlier for normal-tapered P(I-IS-S) and for inverse-tapered P(I-SI-S) copolymers with overall PI volume fractions of 0.35 and 0.33, respectively.[17] TEM studies on related tapered copolymers are in excellent agreement with the SAXS morphologies.[12]

SAXS data from all samples in Table 2 were used to construct the phase diagram shown in **Figure 4**. The phase diagram depicts large areas with the lamellae and HPC morphologies and a smaller area with the bicontinuous/gyroid morphology. Interestingly, the weakly ordered CYL/PL morphologies comprise a large part of the phase diagram that is significantly extended in comparison to sequential P(S-*b*-I) copolymers (Δf range from 0.03 to ≈0.06 in the sequential and tapered copolymers, respectively). On the other hand, the composition range for the bicontinuous/gyroid morphologies is similar in the two systems ($0.64 < f_{PI} < 0.68$).

3.2. Rheology

Changes in the morphology of block copolymers are generally accompanied by distinct changes in the mechanical properties. Accordingly, rheology is a sensitive tool to discern different phases, due to the large viscoelastic contrast of the disordered and the different ordered phases.[6,11,18–23] In addition, the frequency dependence of the storage (G') and loss (G'') shear moduli can provide additional information on the morphology.[18–22] Isochronal measurements of the storage modulus were performed at low frequencies, in the linear viscoelastic region, by slowly heating and cooling, in order to detect the different morphologies and to guide the selection of temperatures for the imminent isothermal measurements. **Figure 5** provides representative results of the isochronal measurements of the storage modulus at $\omega = 1$ rad s^{-1} obtained on heating for some of the tapered copolymers in Table 2. The tapered diblock copolymer SI-253-43 ($f_{PI} = 0.43$) and the copolymer SI-118-73 ($f_{PI} = 0.73$), are in the LAM and HPC morphologies (SAXS). Their storage modulus exhibits nearly constant values following a drop at the PS glass temperature at

© 2022 The Authors. Macromolecular Chemistry and Physics published by Wiley-VCH GmbH

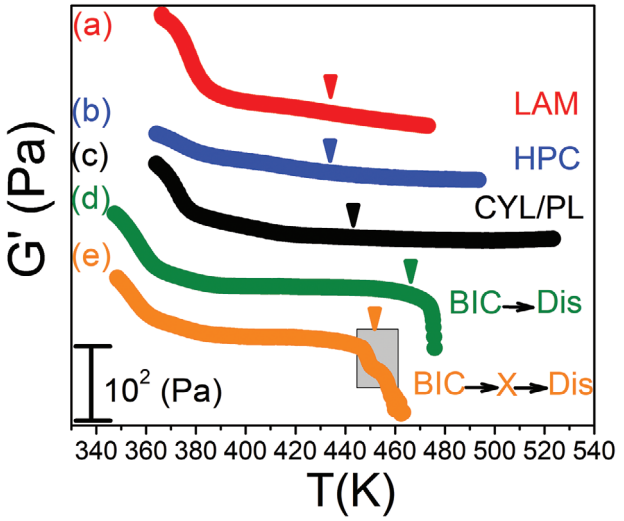

Figure 5. Storage shear modulus during heating (red symbols) for: a) a diblock copolymer SI-253-43, b) SI-118-73, c) SI-97-69, d) SI-51-67, and e) SI-46-68 with a rate of 1 K min^{-1}. A frequency of 1 rad s^{-1} and a strain amplitude of 0.3% were used in all cases. Arrows indicate the temperatures at which the frequency dependent measurements were made (Figure 6).

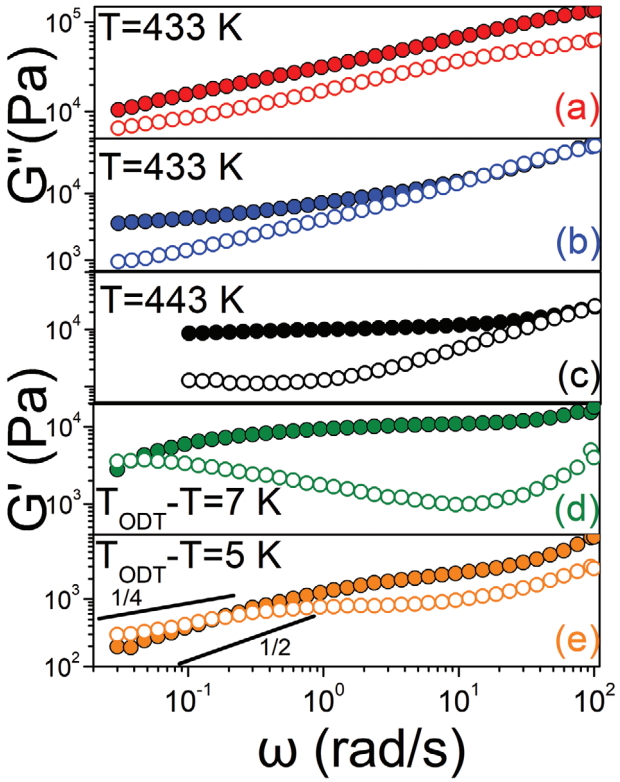

Figure 6. Storage (filled symbols) and loss (open symbols) shear moduli as a function of frequency for cases a–e) corresponding to LAM, HPC, CYL/PL, irregular bicontinuous, and X phases, respectively at the indicated temperatures. Lines with slopes of 1/4 and 1/2 are shown as guides to the eye.

lower temperatures. The $G(T)$ for the SI-97-69 copolymer with the CYL/PL morphology reveals constant values up to the degradation temperature without any sign of disordering. The figure includes the *"G"*(T) dependence for the SI-51-67 copolymer with the LAM morphology up to 413 K and the bicontinuous morphology at higher temperatures up to disordering (the order-to-disorder transition temperature is estimated from rheology at 475 ± 2 K). Several studies on sequential diblock copolymers demonstrated the unique rheological signature of the double gyroid phase with an elastic response ($G' > G$*"*) and an increasing modulus on heating.[17–22] Herein, the system exhibits an elastic response, and the $G'(T)$ dependence within the bicontinuous phase (Figure 5) shows a slight increase on heating up to disordering. On cooling, the phase with the bicontinuous morphology is the only structure, indicating the very slow transformation kinetics to the lamellar phase. Such slow kinetics involving transformation of the Ia$\bar{3}$d phase have been observed in earlier studies.[21,22,24] The copolymer SI-46-68 exhibits an irregular bicontinuous morphology up to 433 K in SAXS, but there exists an additional feature in the isochronal shear modulus at higher temperatures and before disordering (the order-to-disorder transition temperature is estimated from rheology at 458 ± 2 K in comparison to 453 ± 5 K in SAXS). In the majority of studied systems,[4] the Ia$\bar{3}$d phase is the last phase, before disordering occurs.[17–22] Herein, an extra phase (called phase X) appears between the bicontinuous and disordered phases within a small temperature interval ($\Delta T \approx 10$ K). In addition, the cooling curve reveals some hysteresis in the formation of phase X, suggesting its equilibrium character. We mention here that a similar finding was shown by rheology in a sequential SI copolymer ($M_n = 38\,700$ g mol^{-1}) just before disordering.[17] This feature was attributed to a cylindrical morphology. More information about phase X will be provided below, with respect to the isothermal measurements.

More information on the viscoelastic properties of each phase can be extracted from the frequency dependence of the shear moduli. It is well documented that each phase has a distinct viscoelastic fingerprint.[17–25] **Figure 6** depicts the result of isothermal measurements of the storage and loss shear moduli as a function of frequency for (a) the symmetric tapered diblock copolymer SI-253-43, (b) SI-118-73, (c) SI-97-69, (d) SI-51-67, and (e) SI-46-68. The structure assignment of each phase in the copolymer was made by SAXS.

The linear viscoelastic properties of nanophase segregated copolymers have been the subject of theoretical studies. Rubinstein and Obukhov[26] showed that the low frequency response of an orientational disordered lamellar mesophase is dominated by the collective diffusion of the macromolecules along the interface. This mechanism is controlled by defects in lamellar orientation. The high frequency response is ascribed to the dispersion and the number of entanglements of a chain in the interpenetration zone. Kawasaki and Onuki[27] related the lamellar morphology of diblock copolymers to the smectic phase of liquid crystals and found that overdamped second-sound modes in a lamellar phase could result in a dependence of $G^* \approx (i\omega)^{1/2}$. Case (a) corresponds to the viscoelastic response of a lamellar phase where the low-frequency moduli, exhibit weak frequency dependence ($G' \approx \omega^{1/3}$). This dependence lies between the limits of $\omega^{1/2}$ for a disordered lamellar mesophase (for symmetric diblock copolymers) to $\omega^{1/4}$ for the cylindrical mesophase. The weak frequency dependence results from the appearance of an ultra-slow relaxation process related to morphological rearrangements.[4,5] The

© 2022 The Authors. Macromolecular Chemistry and Physics published by Wiley-VCH GmbH

HPC cylindrical phase (b) is characterized by a viscoelastic response. At high frequencies, $G(\omega) \approx G(\omega)$ and both moduli exhibit a weak frequency-dependence, whereas at low frequencies a distinct morphology plateau is observed. The CYL/PL morphology (c) exhibits a similar frequency dependence. Within the bicontinuous phase (d), at a temperature of 7 K below the T_{ODT}, the plateau in $G(\omega)$ and the minimum in $G(\omega)$, reveal an elastic response. At low frequencies, the moduli tend to cross each other to a nonterminal regime, in agreement with earlier studies on the gyroid phase.[21,25] On the other hand, the phase indicated as X (e) exhibits a distinctly different viscoelastic behavior with a crossover in $G'(\omega)$ and $G''(\omega)$ to a nonterminal regime. To obtain addition structural information on this intermediate phase we followed the copolymer structure factor by SAXS (Figure S9, Supporting Information). On heating from the bicontinuous phase the second Bragg peak disappears at temperatures from 443 to 448 K and the system disorders at 453 K. At such intermediate temperatures corresponding to the X phase, the SAXS curves show two components; a narrower component on top of a broad liquid-like peak indicating weak short-range order. In addition, within the X-phase the thermal expansion coefficient, extracted from the temperature dependence of the primary structure factor peak, is weaker as compared to the bicontinuous phase. The above suggest that phase X is a weakly-ordered and fluctuation-controlled phase with a viscoelastic response that separates the bicontinuous from the disordered phase. Because of the weak ordering a structural assignment is not possible at present.

Overall, the phase diagram of tapered copolymers bears similarities to the copolymers made sequentially. However, the reduced interaction parameter creates interfacial mixing giving rise to a broad range of weakly ordered CYL/PL morphologies. This further suggests that the order-to-disorder transition is weakly 1st order with pre-existing concentration fluctuations. Indeed, related results[28] on the ordering kinetics of tapered copolymers revealed increased metastability, as well as slow and even bimodal kinetics in contrast to sequential diblock copolymers. The increased metastability and the defected lamellae mirror the reduced interaction parameter and the weakly ordered morphologies in the tapered copolymers.

4. Conclusion

The phase state in tapered diblock copolymers shows some similarities and some distinct differences from the respective block copolymers made sequentially. The phase diagram consists of the same phases found in sequential block copolymers, i.e., the LAM, HPC, CYL/PL and bicontinuous phases. However, the weakly ordered CYL/PL morphologies comprise a larger part of the phase diagram that is significantly extended in comparison to P(I-*b*-S) copolymers (Δf range from 0.03 to ≈0.06 in the sequential and tapered copolymers, respectively). On the other hand, the composition range for the bicontinuous/gyroid morphologies is similar in the two systems ($0.64 < f_{PI} < 0.68$). These finding are expected to enhance metastability and to slow down the ordering kinetics of tapered copolymers.

Gradient or tapered block copolymers offer a versatile approach toward tunable physical properties. Controlling the tapered interface allows access to higher molecular weight materials that still reside in the weak-segregation limit. However, interfacial mixing gives rise to distinct changes in the phase state (weakly ordered CYL/PL morphologies in a larger part of the phase diagram) that were not considered before. This is of importance both in the design of new materials for thermoplastic elastomers and commercial block copolymer applications.

Supporting Information

Supporting Information is available from the Wiley Online Library or from the author.

Acknowledgements

This research was supported by the Hellenic Foundation for Research and Innovation (H.F.R.I.) under the "First Call for H.F.R.I. Research Projects to support Faculty members and Researchers and the procurement of high-cost research equipment grant" (Project Number: 183). The authors thank Dr. Jan Blankenburg for the calculation of the volume composition profile and the corresponding inflection points. They also thank Prof. Markus Gallei and Martina Plank for the TEM investigation.

Open access funding enabled and organized by Projekt DEAL.

Conflict of Interest

The authors declare no conflict of interest.

Data Availability Statement

The data that support the findings of this study are available from the corresponding author upon reasonable request.

Keywords

tapered copolymers, gradient copolymers, phase states, phase diagrams, nanophase separation

Received: January 26, 2022
Revised: February 24, 2022
Published online: April 4, 2022

[1] W. Wang, W. Lu, A. Goodwin, H. Wang, P. Yin, N.-G. Kang, K. Hong, J. W. Mays, *Prog. Polym. Sci.* **2019**, *95*, 1.
[2] K. Knoll, N. Nießner, *Macromol. Symp.* **1998**, *132*, 231.
[3] G. Kraus, C. W. Childers, J. T. Gruver, *J. Appl. Polym. Sci.* **1967**, *11*, 1581.
[4] M. W. Matsen, F. S. Bates, *J. Chem. Phys.* **1997**, *106*, 2436.
[5] N. Hadjichristidis, S. Pispas, G. Floudas, *Block Copolymers. Synthetic Strategies, Physical Properties and Applications*, J. Wiley and Sons Inc, Hoboken, NJ **2002**.
[6] P. Hodrokoukes, G. Floudas, S. Pispas, N. Hadjichristidis, *Macromolecules* **2001**, *34*, 650.
[7] N. Singh, M. S. Tureau, T. H. Epps III, *Soft Matter* **2009**, *5*, 4757.
[8] M. Luo, J. R. Brown, R. A. Remy, D. M. Scott, M. E. Mackay, L. M. Hall, T. H. Epps III, *Macromolecules* **2016**, *49*, 5213.
[9] J. R. Brown, S. W. Sides, L. M. Hall, *ACS Macro. Lett.* **2013**, *2*, 1105.
[10] J. R. Brown, Y. Seo, S. W. Sides, L. M. Hall, *Macromolecules* **2017**, *50*, 5619.

 © 2022 The Authors. Macromolecular Chemistry and Physics published by Wiley-VCH GmbH

[11] M. Steube, T. Johann, E. Galanos, M. Appold, C. Rüttiger, M. Mezger, M. Gallei, A. H. E. Müller, G. Floudas, H. Frey, *Macromolecules* **2018**, *51*, 10246.
[12] M. Steube, T. Johann, H. Hübner, M. Koch, T. Dinh, M. Gallei, G. Floudas, H. Frey, A. H. E. Müller, *Macromolecules* **2020**, *53*, 5512.
[13] M. Steube, T. Johann, M. Plank, S. Tjaberings, A. H. Gröschel, M. Gallei, H. Frey, A. H. E. Müller, *Macromolecules* **2019**, *52*, 9299.
[14] S. Quinebèche, C. Navarro, Y. Gnanou, M. Fontanille, *Polymer* **2009**, *50*, 1351.
[15] M. Steube, M. Plank, M. Gallei, H. Frey, G. Floudas, *Macromol. Chem. Phys. 222*, **2021**, 2000373.
[16] C. Wahlen, J. Blankenburg, P. Von Tiedemann, J. Ewald, P. Sajkiewicz, A. H. E. Müller, G. Floudas, H. Frey, *Macromolecules* **2020**, *53*, 10397.
[17] R. Roy, J. K. Park, W.-S. Young, S. E. Mastroianni, M. S. Tureau, T. H. Epps, *Macromolecules* **2011**, *44*, 3910.
[18] S. Foerster, A. K. Khandpur, J. Zhao, F. S. Bates, I. W. Hamley, A. J. Ryan, W. Bras, *Macromolecules* **1994**, *27*, 6922.
[19] A. K. Khandpur, S. Foerster, F. S. Bates, I. W. Hamley, A. J. Ryan, W. Bras, K. Almdal, K. Mortensen, *Macromolecules* **1995**, *28*, 8796.
[20] I. W. Hamley, M. D. Gehlsen, A. K. Khandpur, K. A. Koppi, J. H. Rosedale, M. F. Schulz, F. S. Bates, K. Almdal, K. Mortensen, *J. Phys II* **1994**, *4*, 2161.
[21] G. Floudas, R. Ulrich, U. Wiesner, *J. Chem. Phys.* **1999**, *110*, 652.
[22] G. Floudas, B. Vazaiou, F. Schipper, R. Ulrich, U. Wiesner, H. Iatrou, N. Hadjichristidis, *Macromolecules* **2001**, *34*, 2947.
[23] E. Galanos, E. Grune, C. Wahlen, A. H. E. Müller, M. Appold, M. Gallei, H. Frey, G. Floudas, *Macromolecules* **2019**, *52*, 1577.
[24] G. Floudas, R. Ulrich, U. Wiesner, B. Chu, *Europhys. Lett.* **2000**, *50*, 182.
[25] J. Zhao, B. Majumdar, M. F. Schulz, F. S. Bates, K. Almdal, K. Mortensen, D. A. Hajduk, S. M. Gruner, *Macromolecules* **1996**, *29*, 1204.
[26] M. Rubinstein, S. P. Obukhov, *Macromolecules* **1993**, *26*, 1740.
[27] K. Kawasaki, A. Onuki, *Phys. Rev. A* **1990**, *42*, 3664.
[28] E. Galanos, M. Steube, H.-J. Butt, H. Frey, G. Floudas Ordering Kinetics in Tapered Copolymers Based on Isoprene and Stryrene, accepted, J. Chem. Phys. 2022, unpublished.

 © 2022 The Authors. Macromolecular Chemistry and Physics published by Wiley-VCH GmbH